Ezrin NH_2-Terminal Domain Inhibits the Cell Extension Activity of the COOH-Terminal Domain

Marianne Martin, Christophe Andréoli, Alain Sahuquet, Philippe Montcourrier, Marianne Algrain,* and Paul Mangeat

Dynamique Moléculaire des Interactions Membranaires, Centre National de la Recherche Scientifique, Unité de Recherche Associée 1856, Université Montpellier II, 34095 Montpellier Cedex 5, France; and *Biologie des Membranes, Institut Pasteur, 75015 Paris, France

Abstract. Overexpression in insect cells of the full coding sequence of the human membrane cytoskeletal linker ezrin (1-586) was compared with that of a NH_2-terminal domain (ezrin 1-233) and that of a COOH-terminal domain (ezrin 310-586). Ezrin (1-586), as well as ezrin (1-233) enhanced cell adhesion of infected Sf9 cells without inducing gross morphological changes in the cell structure. Ezrin (310-586) enhanced cell adhesion and elicited membrane spreading followed by microspike and lamellipodia extensions by mobilization of Sf9 cell actin. Moreover some microspikes elongated into thin processes, up to 200 μm in length, resembling neurite outgrowths by a mechanism requiring microtubule assembly. Kinetics of videomicroscopic and drug-interference studies demonstrated that mobilization of actin was required for tubulin assembly to proceed. A similar phenotype was observed in CHO cells when a comparable ezrin domain was transiently overexpressed. The shortest domain promoting cell extension was localized between residues 373-586. Removal of residues 566-586, involved in in vitro actin binding (Turunen, O., T. Wahlström, and A. Vaheri. 1994. *J. Cell Biol.* 126:1445–1453), suppressed the extension activity. Coexpression of ezrin (1-233) with ezrin (310-586) in the same insect cells blocked the constitutive activity of ezrin COOH-terminal domain. The inhibitory activity was mapped within ezrin 115 first NH_2-terminal residues. We conclude that ezrin has properties to promote cell adhesion, and that ezrin NH_2-terminal domain negatively regulates membrane spreading and elongation properties of ezrin COOH-terminal domain.

EZRIN (Bretscher, 1983, 1989; Gould et al., 1986, 1989; Turunen et al., 1989) is a member of an expanding family of proteins involved in interactions of the actin cytoskeleton with the plasma membrane at specific cellular locations (Conboy et al., 1986; Rees et al., 1990; Lankes and Furthmayr, 1991; Funayama et al., 1991; Sato et al., 1992), as well as in signal transduction (Gu et al., 1991; Yang and Tonks, 1991) and in growth control (Hunter and Cooper, 1981; Trofatter et al., 1993; Rouleau et al., 1993; Fazioli et al., 1993). Among this family of proteins, moesin, radixin, and merlin/schwannomin, are highly related to ezrin and constitute a subfamily termed ERM proteins (Sato et al., 1992; Bretscher, 1993; Tsukita et al., 1993; Takeuchi et al., 1994*a*). Ezrin is a phosphoprotein with multiple phosphorylation sites and the target of various protein kinases (Hunter and Cooper, 1981; Bretscher, 1989; Urushidani et al., 1989). Transient tyrosine phosphorylation correlated with membrane ruffling activity in A431 cells after EGF stimulation (Bretscher, 1989). Two major sites for tyrosine phosphorylation have been mapped at Tyr 146 and Tyr 354 (Krieg and Hunter, 1992). Interestingly, one is located in the COOH-terminal domain, the other in the NH_2-terminal domain. Via these two domains, ezrin plays a role of a membrane cytoskeletal linker (Hanzel et al., 1991; Algrain et al., 1993), predominant in membrane microvilli and ruffles (Bretscher, 1983, 1989). A regulatory function was also proposed in the massive membrane translocation occurring in acid-secreting gastric parietal cells (Hanzel et al., 1991). Recently identified as a tumor transplantation antigen, ezrin overexpression might confer proliferative advantage on certain tumors (Fazioli et al., 1993).

Ezrin colocalizes in cells with actin-containing structures, and an actin-binding site was recently identified in vitro within ezrin 34 COOH-terminal amino acids (Turunen et al., 1994). Ezrin is highly expressed in gastric parietal microvilli (Hanzel et al., 1991), whereas no gastric protein related to intestinal villin or fimbrin was identified to govern microvilli biogenesis. Therefore, ezrin may exert some other function(s) than a unique structural role of membrane cytoskeletal linker. In one approach, overexpressed ezrin incorporated readily into dorsal microvilli of transfected fibroblasts, but no obvious morphogenic or biogenic action

Please address all correspondence to Dr. Paul Mangeat, Dynamique Moléculaire des Interactions Membranaires, CNRS URA 1856, Université Montpellier II, Bâtiment 24, CC107, place Eugène Bataillon, 34095 Montpellier Cedex 5, France. Tel.: 33 67 14 4725. Fax: 33 67 14 4727.

of ezrin was observed (Algrain et al., 1993). Using an antisense methodology, Takeuchi et al. (1994*b*) demonstrated the cooperative action of ERM proteins in microvilli formation. Moreover, cells lacking ezrin were affected in cell adhesion properties, a result that correlated with the observation that ERM molecules interacted with the hyaluronan receptor CD44 (Tsukita et al., 1994).

Expression of a protein in insect cells using baculovirus is a common mode to produce recombinant proteins. Baculoviral expression of proteins also allows to directly document their physiological functions in infected insect cells. It was particularly useful to discriminate between the various specificities of tau and MAP2 proteins involved in microtubule assembly (Knops et al., 1991; Chen et al., 1992). Brady-Kalnay et al. (1993) made a key observation on the properties of PTPμ in infected insect cells. This receptor-type protein tyrosine phosphatase induced cell aggregation by homophilic binding, a property that was expected with respect to its amino acid sequence homology with adhesion molecules of the immunoglobulin superfamily. This expression system is also useful to study the interaction between different proteins coexpressed in a same cell. That was particularly efficient to study the regulation of $p34^{cdc2}$ activity with cyclin (A and B) and $p107^{wee1}$ (Parker et al., 1991). The effects of overexpression of ezrin could be studied in insect cells as well. Here, we show that human ezrin and, especially, the COOH-terminal domain of the protein promote cell adhesion of virally infected insect cells, induce membrane spreading and extension of elongated cellular processes by mobilization of both actin and tubulin. In addition, we demonstrate that ezrin 115 NH_2-terminal amino acids inhibit the cell extension activity of the COOH-terminal domain of ezrin.

Materials and Methods

Materials

Chemicals were from Sigma Chimie (St. Quentin Fallavier, France). Culture media were from GIBCO BRL (Cergy Pontoise, France). Enzymes and DOTAP transfection-reagent were from Boehringer Mannheim (Meylan, France). Linkers were from New England Biolabs and BacPAK6 virus from Clontech (Ozyme, Montigny Le Bretonneux, France).

Constructions of Baculovirus Transfer Vectors

The baculovirus transfer vector used in this study was one of the pGmAc series described by Royer et al. (1992) in which the polyhedrin start codon was mutated (ATT instead of ATG) and a cloning SmaI (XmaI) site was introduced at a deletion between nucleotides +45 and +462. This pGmAc34T vector and a smaller subclone pEMBL19$^+$/34T, containing the SalI–KpnI polyhedrin gene fragment in the corresponding sites of the pEMBL19$^+$ plasmid (Dente et al., 1983) were further modified by introduction of an NheI linker at the T4 DNA polymerase-treated KpnI site. All the various ezrin constructs were made primarily in the modified pEMBL19$^+$/34T plasmid (hereafter named p34T) rather than in the 9.3-kb pGmAc34T vector because the former plasmid was easier to use and allowed the possibility to produce single-stranded DNA suitable for in vitro mutagenesis. Except when indicated, the EcoRV–NheI fragments, containing the polyhedrin promoter and the different modified ezrin cDNAs, were then introduced in the corresponding sites of the pGmAc34T modified transfer vector. The resulting plasmids were used in the cotransfection procedure with the AcMNPV wild-type DNA to obtain the corresponding recombinant baculoviruses. To obtain the C3Δ21 recombinant virus (see below), Bsu36I-digested BacPAK6 viral DNA was used instead of AcMNPV wild-type DNA in the cotransfection procedure (Kitts and Possee, 1993). In this case the transfer vector was the pM34T plasmid, a derivative of our p34T vector with 3′ additional polyhedrin sequence (fragment KpnI–BamHI), which contained ORF 1629 sequence required to rescue Bsu36I-digested BacPAK6 viral DNA for selection of recombinant baculoviruses.

Constructions of Plasmids Containing Total Ezrin cDNA and its Truncated COOH-Terminal Domains

Human ezrin cDNA was obtained from plasmid pCV6 (Turunen et al., 1989). We would like to mention that a point mutation in codon 286 of ezrin cDNA sequence originating from the pCV6 plasmid was detected by sequencing analysis. This mutation converted a glycine into serine. To use the wild-type ezrin sequence, the correct sequence from the pCV1 plasmid (Turunen et al., 1989) was picked up and reintroduced in the right location of the ezrin cDNA. Thus, all the constructs presented here were made with the wild-type ezrin sequence. A baculovirus expressing the mutated ezrin (EzTSer) was also produced. It gave similar results as the baculovirus producing wild-type ezrin (EzT)[1] (not shown). A BamHI site created upstream of the ATG codon of ezrin cDNA (Andréoli et al., 1994) enabled construction of the plasmid p34T-EzT by blunt cloning the 2.2-kb BamHI–EcoRI fragment in the XmaI site of the p34T vector, restoring a XmaI restriction site 5′ to the BamHI site (Fig. 1). From this plasmid, the p34T-C3 vector was constructed by deletion of the XmaI fragment. After filling in with Klenow enzyme, an 8-mer NcoI linker (CCCATGGG) was added to reconstitute the reading frame. This created a Met-Gly extension at the NH_2-terminal end of the C3 molecule. To eliminate a potential myristylated C3 form, a (GCCATGGC) NcoI linker was also used to create instead a Met-Ala extension. We thus obtained the p34T-C3Gly and p34T-C3Ala plasmids. The p34T-C6 plasmid was obtained by digestion of the p34T-C3Gly vector by ApaI (Fig. 1). After being blunt-ended with T4 DNA polymerase, the plasmid was cut by NcoI, filled in with Klenow enzyme, and ligated with T4 DNA ligase in order to restore the reading frame. The p34T-ΔBB was obtained by BamHI partial digestion of p34T-EzT. The corresponding pGmAc34T-ezrin transfer vectors were constructed as described below.

The pGmAc34T-C1, -C4, and -C5 transfer vectors (Fig. 1) were obtained, respectively, by digestion of p34T-EzT by BglII, Asp718, and HincII. After filling in by Klenow enzyme when necessary, a NcoI linker was added. These intermediate plasmids were then digested by NcoI and NheI and their respective NcoI–NheI containing ezrin fragments were gel-isolated and cloned in the corresponding sites of the pGmAc34T-C3Gly previously obtained.

A XbaI site was created at the 3′ end of ezrin coding sequence by in vitro mutagenesis of p34T-EzT (Norris et al., 1983) in order to modify the stop codon in the CTGTAACAG sequence by CTCTAGAAG. This p34T-EzTXba vector was used to produce the C7 construct. Briefly, a NcoI linker (GCCATGGC) was inserted after deletion of the 5′ XmaI fragment (p34T-C3AlaXb plasmid) and a stop codon was recreated by deletion of the 3′ end ApaI-XbaI fragment. The EcoRV–NheI fragment from this p34T-C7 plasmid was used to produce the corresponding pGmAc34T-C7 plasmid.

To obtain the pM34T-C3Δ21 transfer vector, the (EcoRV–EcoRI) fragment from p34T-C3Ala was gel purified, and then partially digested by Csp6I. After filling in with Klenow enzyme and digestion by NcoI, the 955-bp (NcoI–Csp6I) fragment, deleted of the nucleotides coding for the 21 COOH-terminal amino acids was gel purified, and subcloned in the p34T-C3AlaXb plasmid, in cohesive NcoI and blunt-ended XbaI sites. This restored a stop codon at the 3′ end of the coding sequence. This intermediate plasmid was then digested with EcoRV and NheI, and the fragment containing part of the polyhedrin promoter, the COOH-deleted C3 cDNA and the 3′ non coding sequence of ezrin cDNA was gel purified and subcloned in the corresponding sites of the pM34T transfer vector (see below).

Constructions of Plasmids Containing NH_2-Terminal Ezrin Domains

N1-, N4-, and N2-containing plasmids were obtained, respectively, by digestion of p34T-EzTXbaI vector by BglII, Asp718, and partial digestion by BamHI. After filling in with Klenow enzyme, an 8-mer NheI linker (GGCTAGCC) was inserted in order to reconstitute a stop codon. These intermediate plasmids were then deleted for their 3′ end NheI–XbaI fragments thus creating the p34T-N1, -N2, and -N4 plasmids. Plasmid p34T-N5 was directly obtained by deletion of the HincII–XbaI fragment from the

1. *Abbreviations used in this paper*: EzT, wild-type ezrin; m.o.i., multiplicity of infection.

p34T-EzTXbaI vector. The corresponding pGmAc34T-EzN transfer vectors were obtained as decribed below.

Insect Cell Culture, Virus Production, and Infection

Spodoptera frugiperda (Sf9) cell culture, cotransfection of transfer vectors with AcMNPV wild-type DNA using DOTAP, and plaque assay screening of recombinant baculoviruses were done as described (Andréoli et al., 1994), except for the C3Δ21 recombinant virus which was obtained by recombination between the Bsu36I-digested BacPAK6 viral DNA and the pM34T-C3Δ21 transfer vector. In this case, plaque assay was performed in the presence of 0.2% X-Gal and 0.08% neutral red as described by Kitts and Possee (1993). Recombinant baculoviruses HK and βHK that express, respectively, the complete rat HK-ATPase (α and β chains) and the β chain of HK-ATPase were described in Martin and Mangeat (1994).

For infection, cells were plated at a density of 3.10^6 cells/25 cm^2 flask. One hour later, cells were infected with viral stocks at a multiplicity of infection (m.o.i.) of 5 and cells were harvested at appropriate times after infection and analyzed by SDS-PAGE and immunoblots.

Transient Transfection in CHO Cells

The ezrin COOH-terminal plasmid described by Algrain et al. (1993) was transfected using DOTAP as recommended by the manufacturer for 6 h in CHO cells cultured in DMEM medium supplemented with 10% FCS. Cells were fixed and analyzed by indirect immunofluorescence 24, 48, and 72 h posttransfection. The transfected cells were recognized by the expression of the eleven amino acids of vesicular stomatitis virus glycoprotein tail which epitope tagged the ezrin construct (Algrain et al., 1993).

Antibodies and Light Microscopy

Antibodies raised against recombinant ezrin and against the NH_2-terminal domain of ezrin were produced in rabbits and characterized by Andréoli et al. (1994). As described by Algrain et al. (1993), anti-ezrin antibody is specific of epitopes located on ezrin COOH-terminal domain (Andréoli et al., 1994). For immunofluorescence studies, cells grown on glass coverslips were fixed for 30 min with 3.7% paraformaldehyde. Permeabilization was achieved with 0.2% Triton X-100 in PBS for 4 min. Fixed and permeabilized cells were successively incubated for 30 min with appropriate primary antibodies, followed by commercially available fluorescent secondary antibodies. F-actin was visualized using rhodamine-phalloidin. Anti-tubulin antibodies, mouse mAb DMA1-A and guinea pig antiserum, were a gift from Dr. Ned Lamb and Dr. Keith Burridge, respectively. Cells were viewed on a Leitz Dialux microscope equipped with epifluorescence and 25×, 50×, 63× oil-immersion lenses. Confocal microscopy was performed on a LEICA confocal laser scanner microscope using a 40× oil-immersion lens.

Scanning Electron Microsocopy

Sf9 cells plated on glass coverslips were fixed with 2% glutaraldehyde, 0.1 M Na cacodylate, pH 7.2, 0.1 M sucrose and processed for scanning electron microscopy (Wollweber et al., 1980) followed by critical point drying with CO_2 and gold sputtering. The cells were observed in a Hitachi S4000 scanning electron microscope at 15 kV.

Videomicroscopy

Sf9 cells plated on glass coverslip and infected for 40 h, at an m.o.i. of 10, were mounted in an incubation chamber on a Reichert Polyvar microscope stage maintained at 27°C with an air curtain blower, and observed with video-enhanced Nomarski optics as described (Mangeat et al., 1990).

Adhesion Experiments

4.10^5 Sf9 cells were plated, in triplicate, in 35-mm Petri dishes and infected, at an m.o.i. of 10, with the various recombinant viruses. At 63 h.p.i., the culture medium was removed and the dishes were washed twice with 2-ml culture medium. The cells were scraped off, recovered in 0.5-ml culture medium and counted.

SDS-PAGE and Western Blots

12.5% SDS-PAGE contained 0.1% bis-acrylamide. Transfers on nitrocellulose membranes and Western blots were performed as described earlier (Mercier et al., 1989), and revealed by using ^{125}I-protein A and autoradiography, or horseradish peroxidase–conjugated secondary antibody and the Amersham Corp. (Arlington Heights, IL) ECL procedure.

Results

Cell Extension Properties of Ezrin COOH-Terminal Domain in Sf9 Cells

In a first series of experiments, recombinant baculoviruses were constructed which expressed, under the control of the polyhedrin promoter, either the entire coding sequence of human ezrin (EzT) or two truncated forms of the protein (N5 coding for amino acids 1-233 and C3 for amino acids 310-586) with respect to the proposed linker role (Algrain et al., 1993) of the NH_2-terminal domain with the plasma membrane and of the COOH-terminal domain with the actin cytoskeleton (Fig. 1). In Sf9 cells infected for 44 h with the different baculoviruses, a high expression of a protein running at the expected molecular weights respective of the EzT, N5, and C3 constructs and cross-reactive with anti-ezrin antibodies was observed (Fig. 2 *A*). Sf9 cells are small spheric cells of moth ovarial origin, whose morphology is usually not drastically affected by virus infection (except a well characterized increase in size diameter). Cells infected with HK and βHK baculoviruses (not shown, see Martin and Mangeat, 1994), or with wild-type AcMNPV or ezrin N5

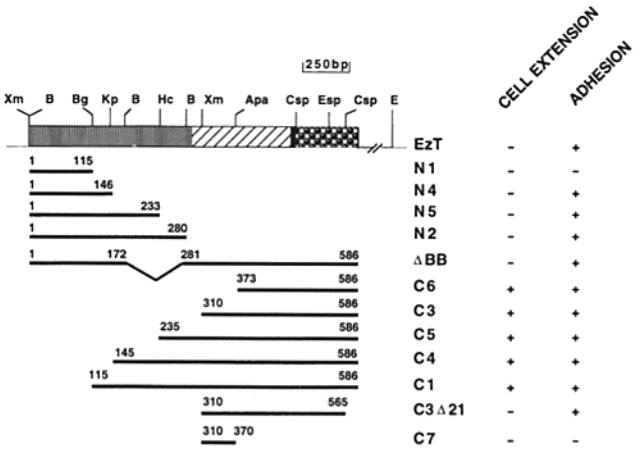

Figure 1. Constructions of the baculovirus transfer vectors used in this study and summary of the effects of the various ezrin constructs expressed in Sf9 cells. Apa, B, Bg, Csp, E, Esp, Hc, Kp, Xm refer, respectively, to sites of cleavage used with the restriction enzymes ApaI, BamHI, BglII, Csp6I, EcoRI, EspI, HincII, KpnI, and XmaI for the different constructions (see Materials and Methods). On the left part of the figure are drawn the various ezrin constructs used. EzT (ezrin 1-586) is presented with successive boxes referring to the various domains of the protein: the NH_2-terminal homologous domain ■, the α-helical motif ▨, the hepta-proline stretch ■, and the COOH-terminal charged motif ■. The untranslated 3′ part of ezrin cDNA inserted in the baculovirus expression vector up to the EcoRI site is indicated by the thin interrupted line. The other constructs are presented as thick solid lines respective of the size and location along the ezrin molecule. The NH_2- and COOH-terminal amino acids of each construct are indicated. On the right part of the figure the effects of expression of the various constructs in Sf9 cells, presented in this study, are summarized.

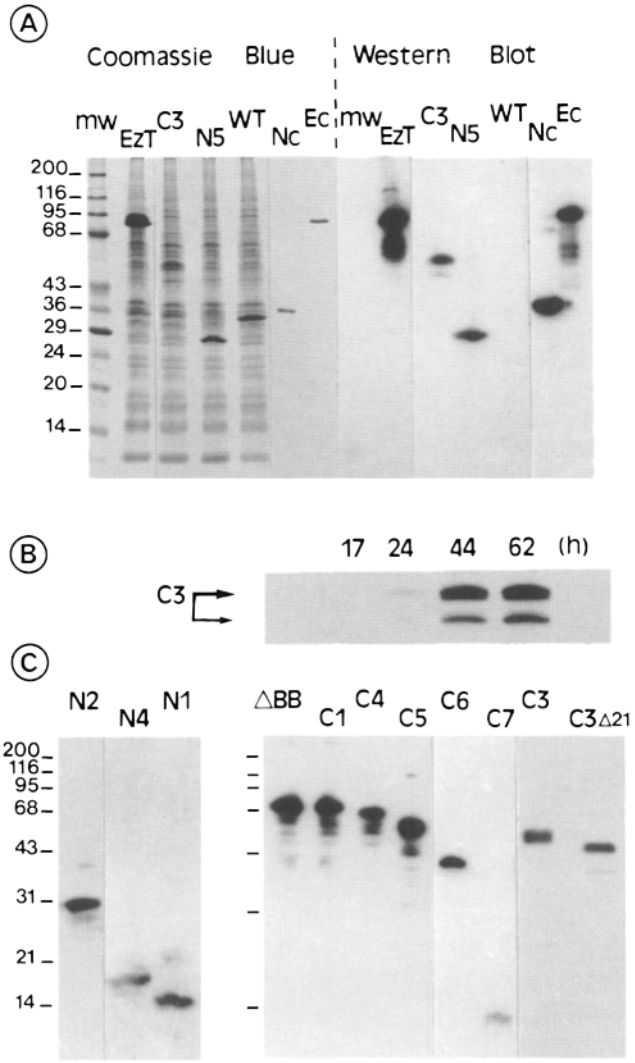

viruses, as well as most of those expressing EzT (Figs. 3 and 4) presented no modification of cell shape. In comparison, the shape of C3-infected cells was drastically modified (Figs. 3–6). These cells presented, at the substratum level, structural modifications characteristic of membrane spreading, lamellipodia, and microspike formation. The morphological modifications were detected 40 h.p.i. (Fig. 4) and were maximal at 63 h.p.i. (Figs. 3 and 5), a time period that correlated with the high levels of expression of C3 in infected cells (Fig. 2 *B*). Qualitatively, cells infected either with C3 or also with EzT or N5 remained more adherent to the plastic or glass substratum than cells infected with wild-type virus (Fig. 3 and see below). In subsequent experiments, the expression of additional ezrin constructs (Figs. 1, 2 *C*, and 7) was assayed in insect cells and was compared with the effects induced by C3 (see later).

Figure 2. Biochemical and immunological characterization of the expression of ezrin and truncated domains in Sf9 cells. A total protein extract equivalent to 10^5 Sf9 cells that were infected for 44 h with different viruses at an m.o.i. of 5, was run on SDS-PAGE and analyzed by Western blotting with a mixture of anti-ezrin and anti-N ezrin antibodies. (*A*) *mw*, molecular weight markers; *EzT*, C3 and N5 correspond to lanes loaded with extract from cells infected with the respective baculoviruses expressing the different ezrin constructs. Note that in this and all subsequent figures, C3 always refers to the C3Gly construct (see Materials and Methods) except when specified differently. *WT*, extract from cells infected with wild-type virus. Nc and Ec refer, respectively, to the recombinant NH_2-terminal domain of ezrin (amino acids 1-308) and total ezrin (1-586) expressed in and purified from *E. coli* and used to prepare antibodies (Andréoli et al., 1994). (*B*) Western blotting of extracts of cells infected with C3 and analyzed at the indicated times postinfection. Note that a C3 degradation product (*lower band*) appeared in this experiment. (*C*) Immunological characterization of additional ezrin constructs by Western blotting. Molecular weight markers are indicated on the left in kD. Note that C3 refers here to the C3Ala construct.

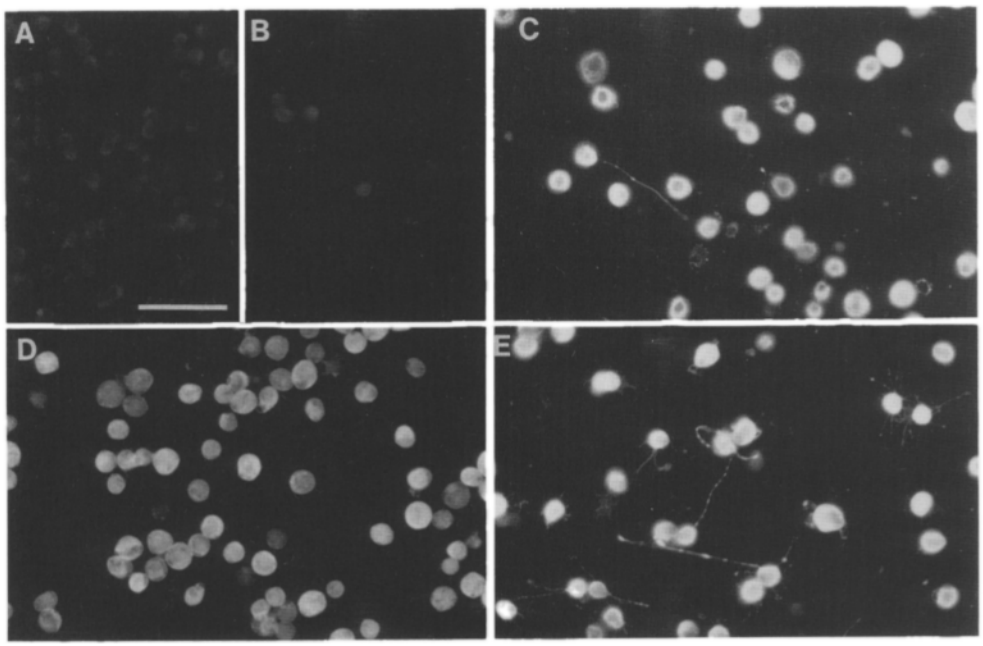

Figure 3. Expression of ezrin and domains in infected insect cells. (*A–E*) Cells plated on glass coverslips (*A*), and infected, at an m.o.i. of 10, with wild-type virus (*B*), EzT (*C*), N5 (*D*), C3 (*E*), were fixed at 63 h.p.i., permeabilized with Triton X-100 and processed for indirect immunofluorescence microscopy. Note that numerous cells in *C*, *D*, and *E*, remained adhesive as compared with cells infected with wild-type virus (*B*). Cells expressing the N5 domain showed no morphological modification, only one cell from those shown in field *C* and that expressed EzT showed one elongated process, whereas most of those expressing C3 presented cell extensions. *A*, *B*, *C*, and *E*, anti-ezrin staining; *D*, anti-N ezrin staining. Bar, 100 μm.

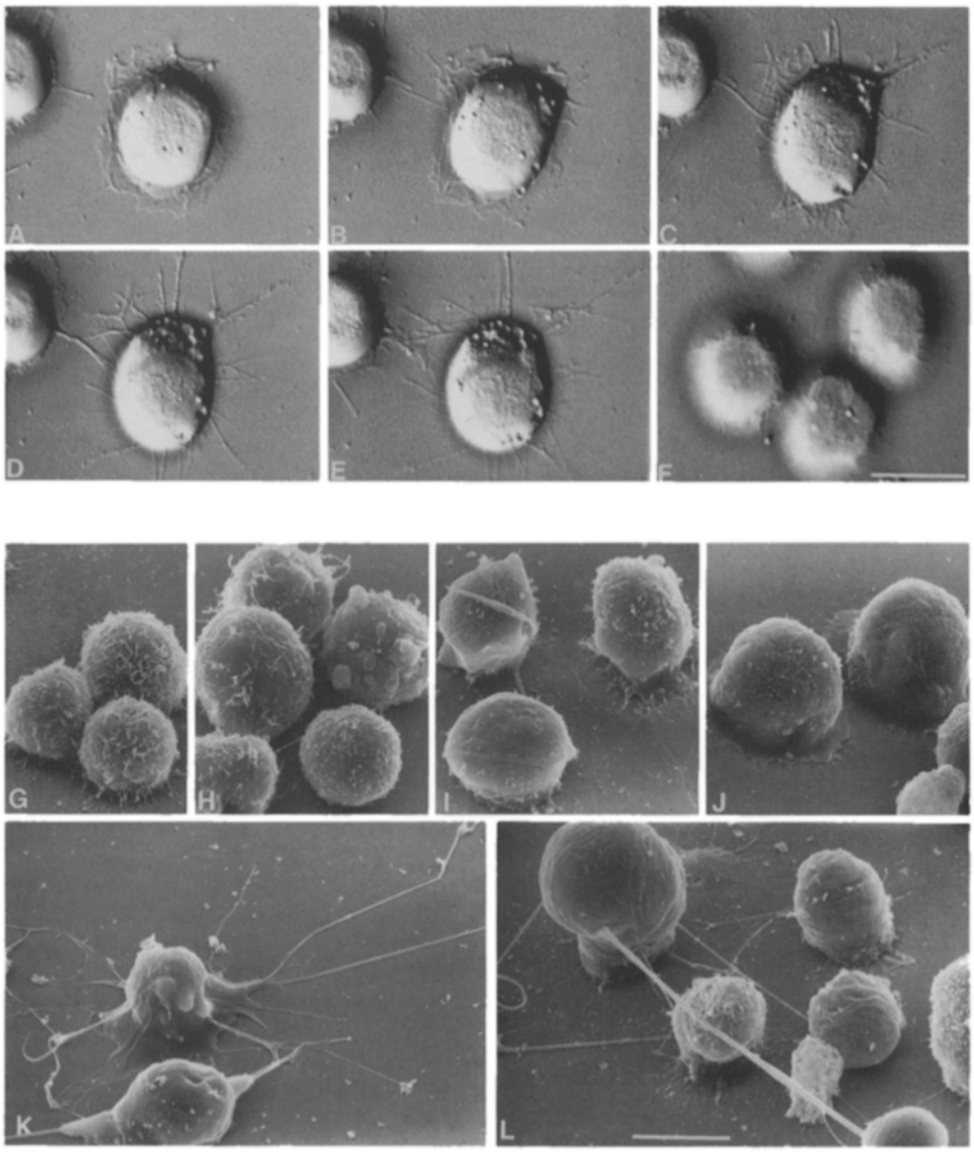

Figure 4. Observations of morphological changes on C3-expressing Sf9 cells by video-enhanced microscopy and scanning electron microscopy. (*A–F*) Live C3-infected cells (*A–E*), plated on glass coverslip, at an m.o.i. of 10, were mounted in an incubation chamber on the microscope stage maintained at 27°C with an air curtain blower and observed with video-enhanced Nomarski optics. Focus was at the substratum level. Although cells were in an upside down position, C3-infected cells (*A*: 40 h.p.i.) appeared in close contact with the substratum. At this time period, a spreading membrane occurred around the cell, whereas most cells infected with wild-type virus began to lose adhesion (not shown). With time (*B*, *C*, *D*, and *E*: 41, 42, 43, and 44 h.p.i., respectively), the spreading membrane of the same cell developed short and highly dynamic microspikes, and then longer and much stabler processes elongated. For comparison, note that live control uninfected Sf9 cells (*F*: focus at the substratum level, as in *A–E*) presented lower spreading properties than C3-infected cells. Bar in *F*: (*A–F*) 20 μm. (*G–L*) Control uninfected Sf9 cells (*G*) or cells infected for 43 h with wild-type virus (*H*), EzT (*I*), N5 (*J*), or C3 (*K* and *L*), at an m.o.i. of 10, were fixed and processed for scanning electron microscopy. Note that the overall morphology of C3-infected cells was greatly different from that of other infected or uninfected cells. C3-infected cells were more adherent and spread than wild-type–infected cells. Most of the processes extending from C3 cells were also adherent to the substratum. Note also that EzT- and N5-infected cells appeared tightly bound to the substratum. Bar in *L*: (*G–L*) 15 μm.

The behavior of live C3-infected cells was followed by videomicroscopy. At 40 h.p.i., wild-type AcMNPV-infected cells started to detach and float in the culture medium. However, the ventral surface of C3-infected cells (Fig. 4, *A–E*) appeared tightly adherent to the substratum whereas even uninfected cells appeared less spreaded (Fig. 4 *F*). A wave of spreading membrane occurred, followed by lamellipodia extension (Fig. 4, *A–E*). Observing live cells, these structures were very dynamic showing phases of continuous growth followed by disruption and growth again. These early dynamic events were totally dependent on actin mobilization since they were immediately blocked when 5 μg/ml cytochalasin D was added to the culture medium (not shown and see later for long term effect of cytochalasin D). From time to time one process adhered more firmly than others to the substratum and a longer extension occurred. These longer processes were developed by steps extending from one adhesive button to another. These latter structures were more stable than shorter lamellipodia and microspikes. Observations with a scanning electron microscope confirmed the anchorage, spreading, and cell extension properties induced in C3-infected cells (Fig. 4, *K–L*).

Ezrin C3 Domain Mobilizes Actin and Tubulin in Sf9 Cells

Endogenous Sf9 actin redistributed into ezrin-containing structures in cells infected with C3 (Fig. 5, *A–C*). Some very long and thin cellular processes (up to 150–200 μm in length) also elongated, clearly adherent to the substratum. Most showed varicosity structures (adhesive buttons), periodically distributed along the length of the process as well as at the terminal tip. These long membrane extensions contained lower levels of actin than shorter lamellipodia (Fig.

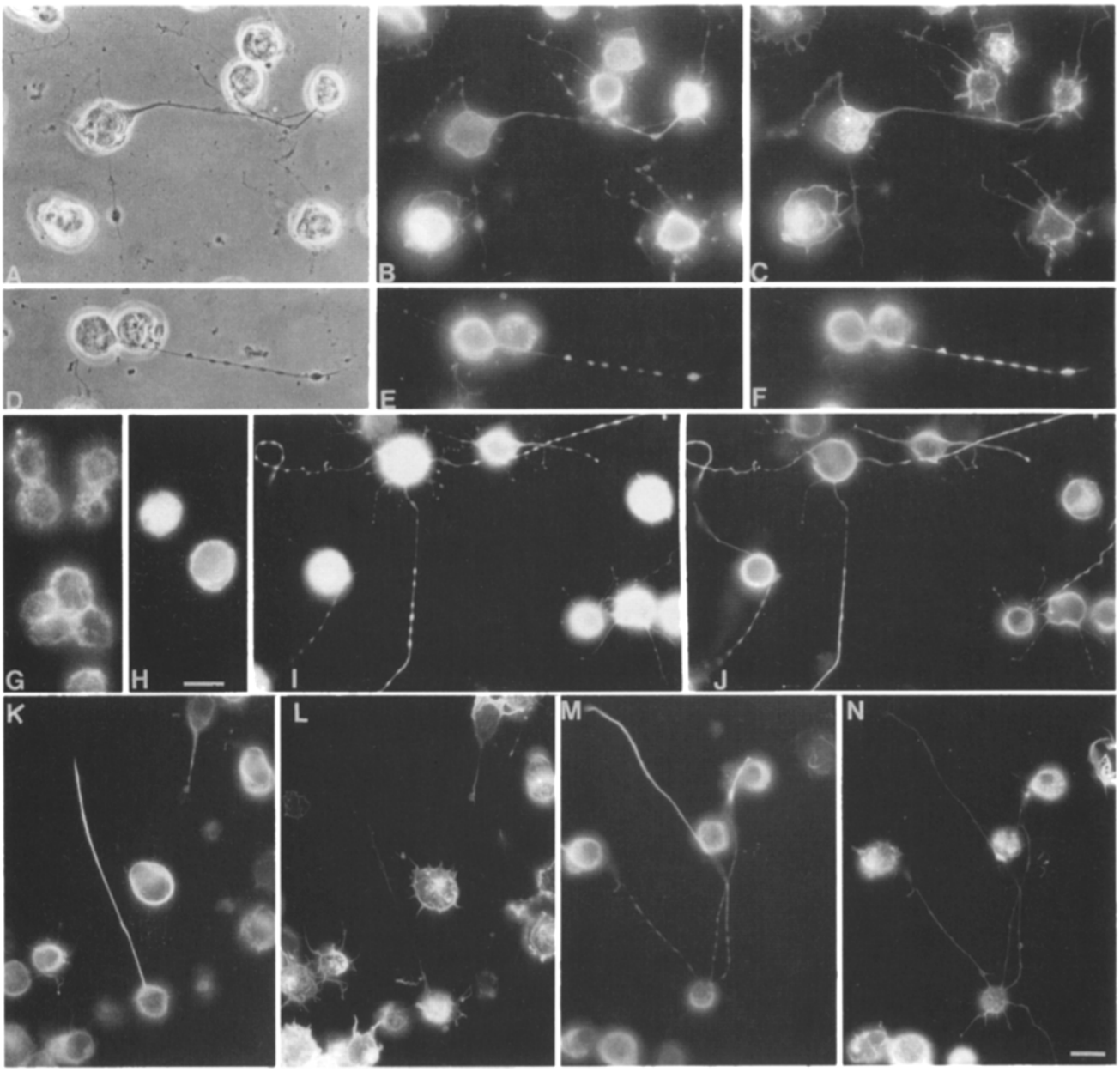

Figure 5. Mobilization of endogenous actin and tubulin in Sf9 cells infected with C3. Sf9 cells plated on glass coverslips were infected for 63 h with C3, at an m.o.i. of 10, (*A–F, I–N*) or with wild-type virus (*H*), or were left uninfected (*G*), and then fixed and processed for double indirect immunofluorescence microscopy after permeabilization with Triton X-100. Cells were stained with either rabbit anti-ezrin affinity-purified antibody (*B, E,* and *I*) or rhodamine-phalloidin (*C, G, H, L,* and *N*) or mouse anti-tubulin mAb (*F, J, K,* and *M*). (*A* and *D*) Phase contrast micrographs of the respective fluorescent fields shown in *B–C* and *E–F. I–J, K–L,* and *M–N* are three different fields doubly labeled. In C3-infected cells, actin was mobilized in the spreading membrane and in the microspikes and was relatively absent from adhesive buttons in long processes. In contrast, tubulin was generally not detected in spreading membranes or short microspikes but was permanent in long processes and stained the adhesive buttons where it colocalized with C3 ezrin. The elongated process of the cell shown in *K–L* was characteristic of the few cells expressing EzT that presented morphologic modifications (as the one shown in Fig. 2 *C*), i.e., these cells generally extended only one long process, intensely labeled with anti-tubulin and mostly devoid of F-actin staining. Bars in *H* (for *A–H*) and in *N* (for *I–N*), 20 μm.

5). Sf9 cell tubulin colocalized with C3 recombinant protein in these structures (Fig. 5, *D–F*). However, most short processes appeared devoid of tubulin staining, but were always positive for F-actin fluorescence. Therefore, actin appeared to be reorganized in association with membrane spreading and microspike formation, before the growth of microtubules into longer adhesive processes. To document further the involvement of actin and tubulin in these effects, drug-interference experiments with microfilament- and microtubule-depolymerizing agents were conducted next.

At 38 h.p.i., a time when enough recombinant protein was synthesized but no obvious morphological effect was yet detected, cells infected with C3 or wild-type viruses, and control uninfected Sf9 cells, were treated with either cytochala-

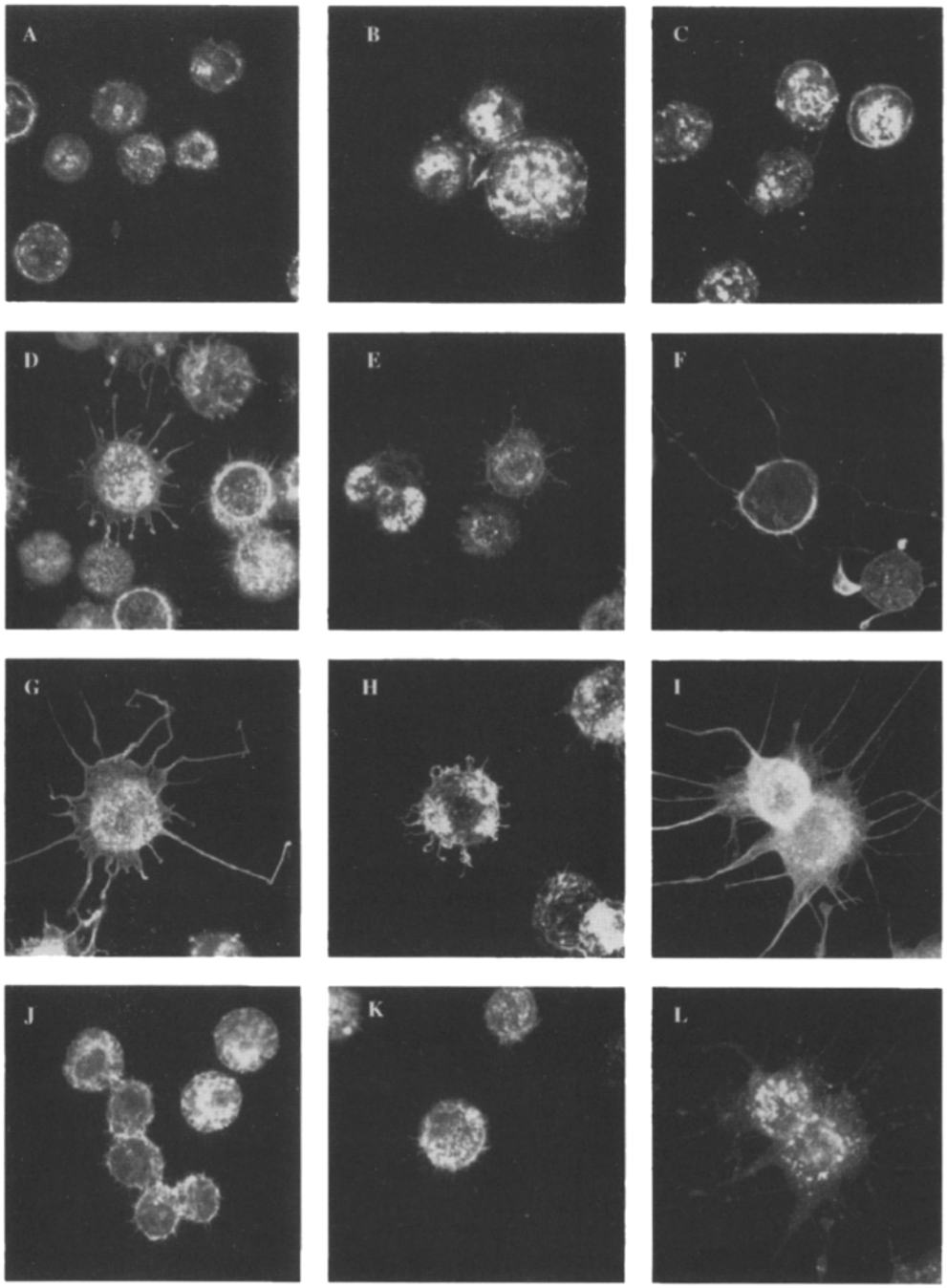

Figure 6. Demicolcine and cytochalasin D effects on uninfected and infected Sf9 cells, a confocal fluorescence microscopy study. Cells infected for 38 h with wild-type virus (*A–C*) or with C3 (*D–H*) or uninfected Sf9 cells (*I–L*) were treated with 20 μM demicolcine (*B*, *E*, *H*, and *K*) or with 5 μg/ml cytochalasin D (*C*, *F*, *I*, and *L*) or left untreated (*A*, *D*, *G*, and *J*). Cells were fixed 6 h (*A–F*, *I–L*) or 22 h (*G* and *H*) later and processed for immunocytochemistry and confocal microscopy. Cells were stained with anti-ezrin (to identify C3-expressing cells, not shown), or with anti-tubulin (*I*) and rhodamine phalloidin (*A–H*, *J–L*). *I* and *L* are the tubulin and F-actin staining of the same field (2 μm thick focal plane). All other fields were shot at the substratum level (0.5 μm focal plane). Note the presence of large ventral patches of F-actin staining in untreated (*D* and *G*) and demicolcine-treated (*E* and *H*) C3-expressing cells, and their absence in cytochalasin-treated (*F*) cells. Each field consisted of a 512 × 512 pixel image (86 × 86 μm wide).

sin D or demicolcine. Treated cells were fixed 6 h or 22 h later and processed for indirect immunofluorescence and confocal microscopy (Fig. 6). Cytochalasin D treatment induced cell extension in all cells, especially in control uninfected Sf9 cells. This was clearly due to mobilization of microtubules (Fig. 6 *I*). Much smaller extensions decorated cells infected with wild-type virus (Fig. 6 *C*), whereas in C3-treated cells (Fig. 6 *F*), extensions were much longer than in C3 control cells (Fig. 6 *D*). In addition, the bright and large patches of F-actin fluorescence which specifically decorated the spreaded ventral surface of these cells, were suppressed in cytochalasin D–treated cells (compare Fig. 6, *D*, *E*, *G*, and *H* with Fig. 6 *F*). Demicolcine treatment of cells affected markedly control uninfected Sf9 cells which readily tend to detach from the substratum. The deficiency in adhesion was less apparent on infected cells. However C3-expressing cells failed to extend long processes (Fig. 6, *E* and *H*). At 60 h.p.i., the cells still presented only short actin-containing microspikes that were observed at the onset of membrane elongation. This experiment demonstrated that further membrane elongation required microtubule assembly.

Amino Acids 566-586 Are Required for the Cell Extension Properties of C3 Domain

To identify further which amino acid sequences of ezrin were responsible for the various effects observed in Sf9 cells, additional recombinant baculoviruses were constructed (Fig. 1)

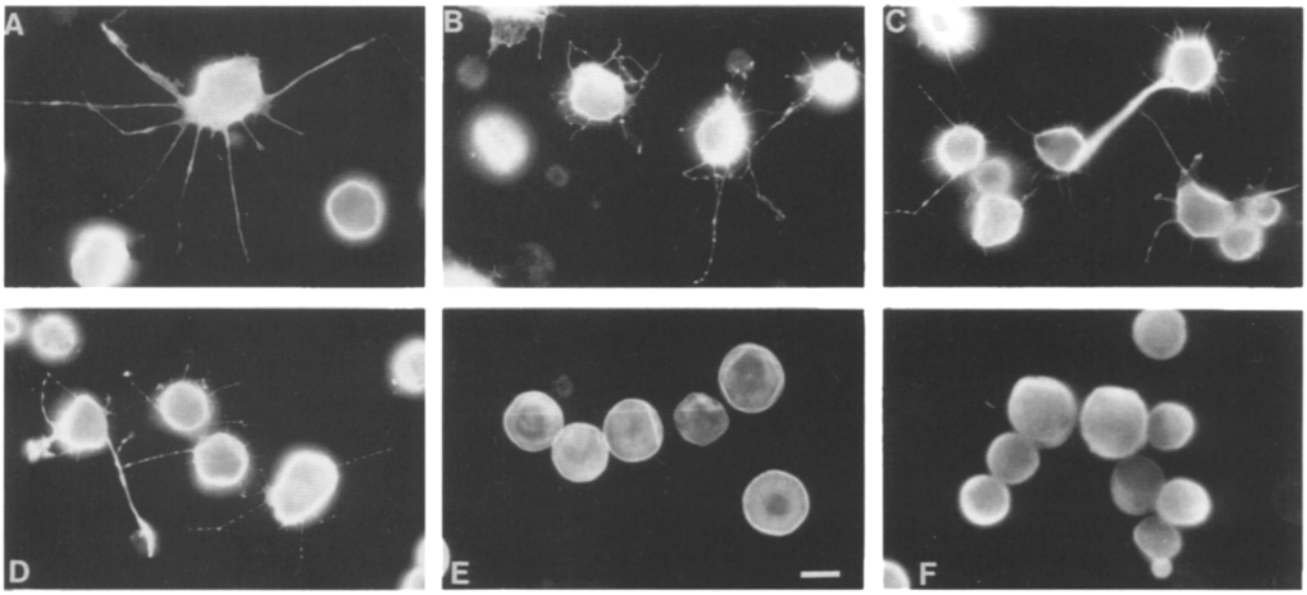

Figure 7. Cell extension effect of C1, C4, C3Ala, and C6 constructs expressed in Sf9 cells. Cells infected, respectively, with C1 (*A*), C4 (*B*), C3Ala (*C*), C6 (*D*), ΔBB (*E*), and C3Δ21 (*F*) were fixed and processed for anti-ezrin immunofluorescence 44 h.p.i. Note that cells infected with ΔBB and C3Δ21 did not induce extensions. Similar results were obtained at 63 h.p.i. (not shown). Bar, 20 μm.

and the various recombinant polypeptides were analyzed by Western blotting (Fig. 2 *C*) and by indirect immunofluorescence microscopy (Fig. 7). A different C3 virus (C3Ala) was also constructed that was slightly different from the first C3 virus used (see Materials and Methods). C3Ala was as effective as C3 to develop cell extension (Fig. 7 *C*) and ruled out that the observed extensions resulted from an artifact, i.e., the presence of a myristylated moiety in the construct. Constructs with NH_2- or COOH-terminal deletions of C3 were prepared to examine which domain of C3 was required for the observed activity. Cell extensions were still observed with the C6 construct that expressed a shortened C3 domain deleted of 62 inactive NH_2-terminal residues (C7 fragment) (Fig. 7 *D*). However, when C3 was deleted from its 21 COOH-terminal amino acids (C3Δ21 construct), cell extension was markedly impaired (Fig. 7 *F*). On the other hand, cell extension was also triggered by a very large construct expressing 4/5 of full ezrin (C1) that contained the COOH-terminal domain and most parts of the NH_2-terminal domain but the 115 first amino acids (N1 domain) of ezrin (Fig. 7 *A*). Interestingly, a construct (ΔBB) that expressed ezrin deleted of a large region of the NH_2-terminal domain but that still contained the first 172 amino acids had no effect (Fig. 7 *E*). Accordingly, no morphological change was observed in cells infected with two additional NH_2-terminal constructs, N4 and N2 (not shown). This implied that ezrin N1 region was a candidate inhibitor of the activity of C3 domain in the whole protein.

Amino Acids 1-115 within Ezrin N5 Inhibit the Cell Extension Activity of the C3 Domain

Since C3 induced cell extension in Sf9 cells, and that was not the case in cells infected with N5 and in most of cells infected with EzT, a possible role of ezrin NH_2-terminal domain to act as a negative regulator of the cell extension activity of the C3 domain was considered. To test this hypothesis, a series of coinfection experiments were performed. Cells were coinfected for 44 h with C3 virus at a constant m.o.i. and with N5 virus at various m.o.i. (Fig. 8). The coexpression of the two proteins in the same cells was controlled by indirect immunofluorescence microscopy, and Western blotting showed that the amount of expression of each protein was about one-half of what was achieved in single infection experiments (Fig. 8 *B*). In coinfected cells, an inhibition of C3 cell extension activity was clearly observed dependent of the level of N5 expression. In cells coinfected with N5 at an m.o.i. of 10 and 30, spreading membrane and cell extension were no more apparent (Fig. 8 *A*). In additional coinfection experiments performed with N1 and C3 viruses, cell extensions were also inhibited (Fig. 8 *C*, pictures *C–D*). The inhibitory effect of N5 and of N1 over the activity of C3 was very specific since coinfections performed with another recombinant virus unrelated to ezrin (βHK, Fig. 8 *C*, pictures *E–F*) or with wild-type virus (not shown) did not prevent cell extension by C3. This experiment suggested that in order to inhibit the activity of C3 domain, amino acids 1-115 of ezrin NH_2-terminal domain might interact with ezrin C3 domain or compete with a same substrate.

Ezrin Enhances Cell Anchorage

From the start of this study, it appeared obvious that expression of ezrin or of various ezrin-truncated forms in Sf9 cells qualitatively affected the adhesion properties of Sf9 cells during the infection period. Ezrin-expressing cells remained adherent for a much longer time than cells infected with wild-type virus or with other recombinant viruses unrelated to ezrin. It was particularly evident for cells that developed extensions as shown in videomicroscopy and scanning electron microscopy observations (Fig. 4). To investigate further, a quantitative measurement was made on cells infected with various viruses for 63 h. As shown in Fig. 9, most forms of

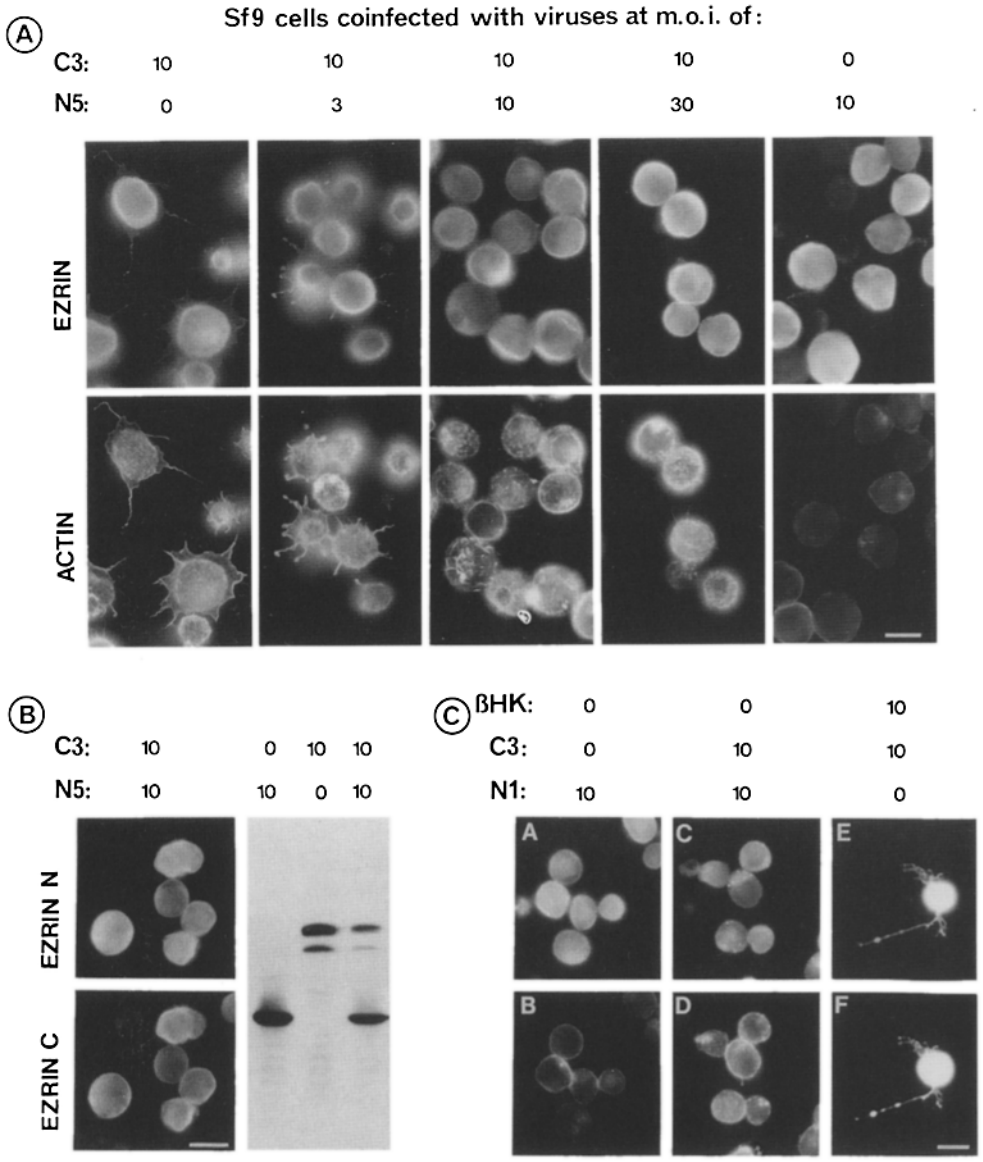

Figure 8. Inhibition of C3 cell extension effect by N5 and N1. (*A*) Sf9 cells were coinfected with C3 and N5 at the indicated m.o.i. for 44 h, fixed, and processed for double-labeling immunofluorescence. The expression of ezrin N5 domain was followed with rabbit anti-N ezrin antibody (*top right picture of A*) whereas the expression of ezrin C3 domain was detected with ezrin antibodies which recognized epitopes only located on the COOH-terminal domain of ezrin (Andréoli et al., 1994). F-actin was stained with rhodamine-phalloidin. Note the drastic extinction of phalloidin fluorescence when cells were simultaneously stained with anti-N ezrin antibody (*bottom picture of A*). In *B* a Western blot of cells infected, as indicated, for 44 h, showed that about half of each recombinant product was recovered in coinfected cells. Double indirect immunofluorescence microscopy using specific antibodies against each ezrin domain (rabbit anti-N ezrin, mouse anti-gastric ezrin mAb specific for the COOH-terminal domain) demonstrated that most of the cells were coinfected. (*C*) Inhibition of C3 cell extension action by N1. Infected Sf9 cells, as indicated, were stained 44 h.p.i. Cells were labeled with anti-N antibodies (*A* and *C*) and rhodamine-phalloidin (*B* and *D*). Note the faint F-actin staining observed in *B*, as compared with *D* when C3 was coexpressed (conditions of time of exposure and printing were identical). (*E–F*) Cells were stained with anti-ezrin (*E*) and anti-βHK-ATPase (*F*) antibodies. In this latter case coexpression of a different protein, βHK-ATPase, together with C3 did not impair the cell extension action of C3. Bar, 20 μm.

ezrin elicited a significant adhesive action on Sf9 cells except those infected with N1 virus, wild-type virus, HK, or βHK. Therefore, the adhesion effect was a specific property of ezrin constructs but was not restricted to domains of ezrin that trigger cell extension but involved also other parts of the molecule, especially most of the NH_2-terminal domain.

The COOH-Terminal Domain of Ezrin Induces Cell Extension in CHO Cells

Although several examples have now been published that prove the reliability of the baculovirus expression system (see introduction), effects observed during high expression of a recombinant human protein in infected insect cells might still be difficult to reconcile with the actual physiological function of the protein. That question was particularly relevant in the case of the COOH-terminal domain of ezrin since the transient expression of a similar construct in CV1 cells did not affect markedly these cells (Algrain et al., 1993). We hypothesized that the plasticity of the cytoskeleton in a particular cell line might influence the cell response to the high expression of ezrin COOH-terminal domain. We found that when CHO cells were transfected with the same plasmid used by Algrain et al. (1993), different effects than those described in CV1 cells were obtained (Fig. 10). In CHO cells, expression of the COOH-terminal domain of ezrin induced drastic morphological modifications of the cells. In cells which expressed low levels of ezrin COOH-terminal domain, most of the protein was incorporated at the tip of an elongated membrane extension (Fig. 10, *A–B*). When higher levels of the construct were expressed the cell morphology was drastically modified. The tranfected cells presented a spheric cell body, generally adherent on top of nontransfected cells, with one or several thin extensions of various

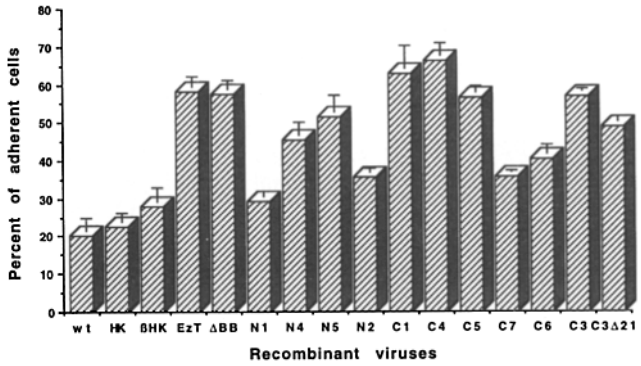

Figure 9. Adhesion properties of ezrin constructs, 4×10^5 cells plated in 35-mm plastic petri dishes were infected, at an m.o.i. of 10, with wild-type virus (*wt*), HK-ATPase (*HK*), βHK-ATPase (*βHK*) and the different ezrin constructs as indicated. At 63 h.p.i., the culture medium was removed and the dishes were washed twice with 2-ml culture medium. The cells were scraped, and recovered in 0.5-ml culture medium and counted. The results, a composite of three different experiments, were expressed as percent of cells recovered as compared with the number of cells plated and represented means of triplicate counts in each experiment. All values, except those of N1, HK, or βHK were significantly different with $p < 0.01$ or better (Student's *t* test) than those obtained with wild-type virus (*wt*). The value of C7 is at the significancy limit. For comparison, control uninfected Sf9 cells had multiplied to a score of 317% during the same period of time.

lengths, which stained for both actin and tubulin. The COOH-terminal domain was mainly incorporated at the cell contour. Some transfected cells showed morphological changes similar to insect cells that expressed ezrin C3 domain (Fig. 10, *G–H*). We concluded that the effect observed in insect cells was reproducible in a mammalian cell line and therefore of general physiological significance.

Discussion

The main result of this study is that, when overexpressed in Sf9 cells, ezrin COOH-terminal domain possesses a constitutive cell extension activity that is inhibited by the NH_2-terminal domain. The expression of the full molecule in Sf9 cells was investigated biochemically and ultrastructurally and the details are published elsewhere (Andréoli et al., 1994). Ezrin accumulated specifically at the plasma membrane and bound in vitro a 77-kD Sf9 cell peripheral membrane protein, which behaved like an ERM-related protein. Self-assembly of ezrin at the plasma membrane by oligomerization involved both NH_2- and COOH-terminal domains (Gary and Bretscher, 1993; Andréoli et al., 1994). It is thus likely that the NH_2-terminal domain of ezrin exerts a regulatory negative control over the activity of the COOH-terminal domain, leading mainly to no morphological alteration in EzT-infected cells. Ezrin C3 domain might therefore act as a dominant-negative mutant that competed with the insect endogenous ERM-like protein(s).

In EzT-infected cells, a direct intra-, and/or inter-, molecular interaction between ezrin NH_2- and COOH-terminal domains might prevent the active conformation of the COOH-terminal domain to take place. Some biochemical evidences support the existence of such interaction (Andréoli et al., 1994). Alternatively, a competition between both domains for the same substrate might occur. The substrate might be actin itself. One actin-binding site was unmasked (Algrain et al., 1993) and identified in vitro in the COOH-terminal domain (Turunen et al., 1994). Still, no actin-binding properties have yet been strongly documented in vitro for the full ezrin molecule. Then it is possible that the NH_2-terminal domain directly inhibits the actin-binding properties of the COOH-terminal domain. At last, the regulatory action of the NH_2-terminal domain over the activity of the COOH-terminal domain might involve a combination of both mechanisms, each being possibly regulated by phosphorylation. This complex aspect of regulation was indirectly apparent in coinfection experiments. An unexpected extinction of rhodamine phalloidin fluorescence was observed in N5 (and N1) expressing cells that were stained with anti-N ezrin antibody (Fig. 8 and unpublished results). This extinction was relieved when both NH_2- and COOH-terminal domains were coexpressed (Fig. 8 *C*). This might tentatively suggest that the spatial location of the NH_2-terminal domain relatively to actin microfilaments in Sf9 cells is dependent on the presence or the absence of ezrin COOH-terminal domain.

Both ezrin NH_2- and COOH-terminal domains, as well as the full protein, enhance the adhesion of infected cells independently of the cell extension activity of the COOH-terminal domain. These results imply that ezrin triggers the reorganization of adhesion proteins at the cell surface to enhance cell anchorage. Since ezrin is normally expressed in the apical membrane of epithelial cells (Berryman et al., 1993), we cannot rule out that this result reflects a side effect of the overexpression approach, that might be related to the actual function of another ERM protein, such as radixin, which is physiologically present in adherens junctions (Sato et al., 1991; Tsukita et al., 1989). However, Tsukita and colleagues recently reported experimental evidences for the involvement of ezrin in adhesion mechanisms. Cells lacking ezrin presented some defect in plating efficiency (Takeuchi et al., 1994*b*) and ERM proteins were found to bind an isoform of CD44, an integral membrane protein that functions as the receptor for hyaluronan (Tsukita et al., 1994). Our present results therefore are well consistent with this new background regarding ezrin functions. If the NH_2-terminal domain is indeed involved in membrane binding via an adhesion molecule, it is not surprising that its overexpression enhances cell adhesion. Accordingly, the adhesion effect related to the COOH-terminal domain might indicate that some amino acid sequence is also involved in membrane binding. Such a site exists for the binding of talin with integrin (Burridge, K., personal communication). Since we had characterized the binding of ezrin on Sf9 cell membranes (Andréoli et al., 1994), it is conceivable that a conserved CD44-like molecule, or another related adhesion molecule, is present in Sf9 cells that might be activated and/or reorganized by the binding of ezrin molecules at the inner face of Sf9 cell membranes leading to a strengthened adhesive property of these cells.

Overexpression of a protein in insect cells is much higher than what is generally achieved during transient transfection experiments. This could have explained why we observed morphological effects with some of the ezrin constructs in contrast to Algrain et al. (1993), who expressed ezrin NH_2- and COOH-terminal domains in CV1 cells. In view of our

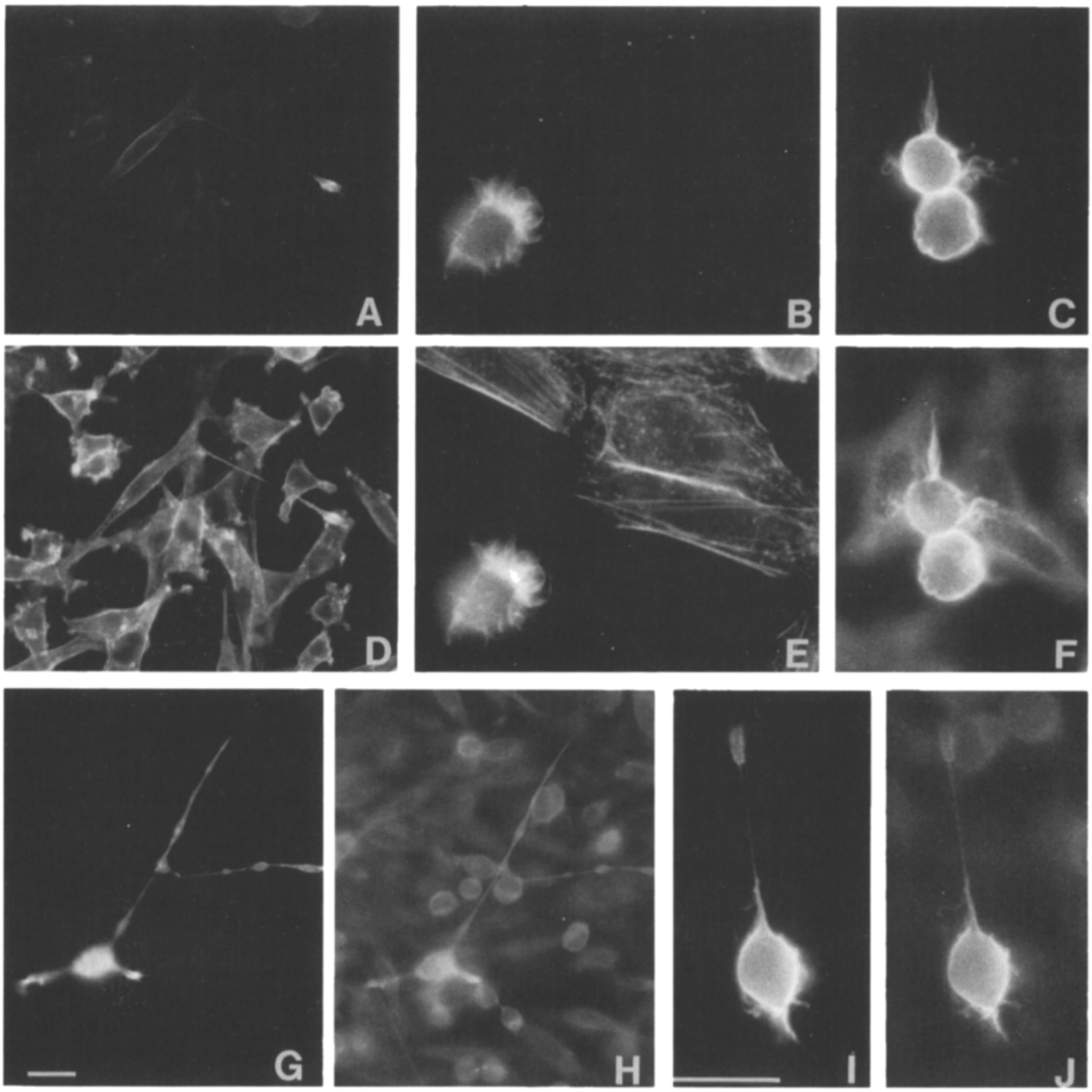

Figure 10. Transient expression of the COOH-terminal domain of ezrin in CHO cells. Cells were transfected with the plasmid described by Algrain et al. (1993) and were fixed and processed for indirect immunofluorescence 72 h later. Cells were doubly stained with anti-mouse mAb directed against the eleven amino acids of the vesicular stomatitis virus glycoprotein tail which epitope tagged the ezrin construct and allowed unambiguous localization of the transfected cDNA product (*A*, *B*, *C*, *G*, and *I*) and with either rhodamine phalloidin (*D*, *E*, and *F*) or with anti-tubulin antibody (*H* and *J*). Note that the transfected cell in *A* expressed a low amount of the COOH-terminal domain, which is concentrated at the tip of an elongated extension. The shape of transfected cells with higher levels of expression was drastically modified (*B*, *C*, *G*, and *I*). The cell body was spheric and several thin extensions developed at one or several poles of the cells. The fluorescence of the epitope tagged ezrin domain was concentrated at the cell contour and colocalized with F-actin (*D*, *E*, and *F*) and tubulin (*H* and *J*). Note that most of transfected cells were recovered on top of nontransfected cells. These latter appeared with a blurred fluorescence, especially in fields *F*, *H*, and *J*. Note the peculiar morphology of the transfected cell in *G* and *H*, which looks like C3-expressing Sf9 cells. Similar results were obtained for cells stained 48 h posttransfection. Bars = 25 μm in *G* for fields *A*, *B*, *G*, and *H* and in *I* for fields *B*, *C*, *E*, *F*, *I*, and *J*.

own transient transfection experiments in CHO cells, it is more likely that the plasticity of infected Sf9 cell cytoskeleton, as well as that of CHO cells, allows ezrin COOH-terminal domain to exert effects that it is incapable of in the presence of the preexisting network of actin stress fibers and microtubules of CV1 cells. Recently, Edwards et al. (1994) described another ERM-like protein, *Drosophila* moesin, which induced changes of cell shape in the fission yeast. Interestingly, this effect was obtained by expression of a truncated form of *Drosophila* moesin containing the COOH-terminal domain. In insect cells infected with a baculovirus, it is well described that actin microfilaments are reorganized

from a subplasmalemma structure to a nuclear location (Volkman et al., 1992). At the same time, microtubules are depolymerized (Volkman and Zaal, 1990) and these events are instrumental in the virus-induced rounding of infected cells. Therefore, ezrin COOH-terminal domain is capable of overcoming the effects of viral infection on both cytoskeletal proteins.

The suppression of the activity of the C3 domain by deletion of the last 21 COOH-terminal amino acid supports a direct effect of ezrin COOH-terminal domain on actin occurs via the binding site independently identified by Turunen et al. (1994). How actin is mobilized is not totally understood. Radixin was described as a barbed-end capping protein (Tsukita et al., 1989), and the actin-binding site is present in a highly conserved amino acid sequence among ERM proteins (Turunen et al., 1994). One could imagine that ezrin C3 domain might act at the barbed-end of actin filaments as well, but additional biochemical data are needed to clear this point. It is unclear to explain how ezrin COOH-terminal domain mobilizes tubulin in insect and CHO cells and whether this is the result of a direct or indirect interaction of ezrin with tubulin. Nonetheless, some elongated processes resemble the outgrowths of axons and dendrites. To our knowledge, expression of only very specific microtubule-associated proteins expected to be involved in the formation of axon and dendrite induced similar extensions, but without adhesive buttons, in insect cells (Knops et al., 1991; Chen et al., 1992). In ezrin C3-expressing cells, the kinetics of occurrence of extensions, and the results of the drug-interference experiments demonstrated that actin mobilization is required for tubulin assembly to proceed. One should notice, however, that the phenotypic effect was obtained when only a truncated ezrin molecule was expressed. Additional experimental information is therefore necessary to assess whether or not ezrin or one ERM-related protein exerts a role in actin/microtubule-associated structures and especially in axonal growth as was previously proposed (Birgbauer and Solomon, 1989; Goslin et al., 1989; Everett and Nichol, 1990; Birgbauer et al., 1991).

The main issue raised by this study is related to the physiological consequences of our observations. It is striking that one domain of ezrin has the constitutive capacity to induce gross morphological changes that are expected to occur at physiological subcellular sites where ezrin is localized (ruffling membranes, parietal cell microvilli, and axonal growth cone). On the other hand, the full molecule is apparently incapable of such effects. Does ezrin C3 act as a dominant-negative mutant or is it possible that an as yet unraveled physiological ezrin activator exists? For example, the elongated processes observed in some EzT cells (Fig. 3 *C*) might be induced by an activated COOH-terminal domain that resulted from proteolytic cleavage of ezrin. Ezrin is, indeed, very sensitive to calcium-dependent proteases, and one could correlate the propensity of ezrin to generate a COOH-terminal domain approximately the same size as C3 domain by calpain cleavage. Yao et al. (1993) tested whether ezrin degradation by calpain, which colocalizes with ezrin in secretory apical microvilli, could be physiologically relevant in gastric parietal cells. However, a significant degradation of gastric ezrin required non-physiological conditions of intracellular calcium. It is therefore more appropriate to determine whether and how the negative regulatory activity of the NH_2-terminal domain is relieved in cells to generate a fully activated molecule. Ezrin NH_2-terminal domain is primarily known as the site responsible for ezrin binding at the membrane (Algrain et al., 1993). Our study demonstrates that it likely exerts other functions, one related to the control of cell adhesion, another to negatively control the activity of ezrin COOH-terminal domain. The physiologic role of ezrin COOH-terminal domain has to be reevaluated as well. Since C3 domain promotes a drastic morphological effect, one obvious conclusion is that this domain may act directly or indirectly on the cell membrane. This observation is strengthened by the enhanced adhesive properties of cells that expressed most of the COOH-terminal constructs, especially that of C3Δ21, which induced no cell extension. It is therefore apparent now that the functions of both domains of ezrin are not simply to bind membrane on one hand and to interact with cytoskeleton on the other hand as previously assumed.

We thank Drs. M. Arpin and D. Louvard for helpful discussion and communication of their results before publication, Dr. A. Vaheri for providing human ezrin cDNA, Drs. M. Cerutti and G. Devauchelle for the pGmAc34T vector and the Sf9 cell line and the conditions of cell culture and cell transfection, Drs. K. Burridge and N. Lamb for the gift of anti-tubulin antibodies and the help of the latter with confocal microscopy, and Dr. J. G. Forte for anti-gastric ezrin mAb.

This work was performed in part in the Centre National de la Recherche Scientifique-Institut National de la Santé et de la Recherche Médicale de Pharmacologie-Endocrinologie in Montpellier, France. Laurent Charvet is acknowledged for the photographic work. This work was supported in part by grants from l'Association pour la Recherche sur le Cancer (contract 6844 to P. Mangeat and fellowship to C. Andréoli), la Ligue Nationale contre le Cancer, la Fondation pour la Recherche Médicale et l'Association Française contre les Myopathies.

Received for publication 24 October 1994 and in revised form 7 December 1994.

References

Algrain, M., O. Turunen, A. Vaheri, D. Louvard, and M. Arpin. 1993. Ezrin contains cytoskeleton and membrane binding domains accounting for its proposed role as a membrane-cytoskeletal linker. *J. Cell Biol.* 120:129–139.

Andréoli, C., M. Martin, R. Le Borgne, H. Reggio, and P. Mangeat. 1994. Ezrin has properties to self-associate at the plasma membrane. *J. Cell Sci.* 107:2509–2521.

Berryman, M., Z. Franck, and A. Bretscher 1993. Ezrin is concentrated in the apical microvilli of a wide variety of epithelial cells whereas moesin is found primarily in endothelial cells. *J. Cell Sci.* 105:1025–1043.

Birgbauer, E., and F. Solomon. 1989. A marginal band-associated protein has properties of both microtubule- and microfilament-associated proteins. *J. Cell Biol.* 109:1609–1620.

Birgbauer, E., J. H. Dinsmore, B. Winckler, A. D. Lander, and F. Solomon. 1991. Association of ezrin isoforms with the neuronal cytoskeleton. *J. Neurosci. Res.* 30:232–241.

Brady-Kalnay, S. M., A. J. Flint, and N. K. Tonks. 1993. Homophilic binding of PTPμ, a receptor-type protein tyrosine phosphatase, can mediate cell-cell aggregation. *J. Cell Biol.* 122:961–972.

Bretscher, A. 1983. Purification of an 80,000-dalton protein that is a component of the isolated microvillus cytoskeleton, and its localization in non muscle cells. *J. Cell Biol.* 97:425–432.

Bretscher, A. 1989. Rapid phosphorylation and reorganization of ezrin and spectrin accompany morphological changes induced in A-431 cells by epidermal growth factor. *J. Cell Biol.* 108:921–930.

Bretscher, A. 1993. Microfilaments and membranes. *Curr. Opin. Cell Biol.* 5: 653–660.

Chen, J., Y. Kanai, N. J. Cowan, and N. Hirokawa. 1992. Projection domains of MAP2 and tau determine spacings between microtubules in dendrites and axons. *Nature (Lond.).* 360:674–677.

Conboy, J., Y. W. Kan, S. B. Shodet, and N. Mohandas. 1986. Molecular cloning of protein 4.1, a major structural element of the human erythrocyte membrane skeleton. *Proc. Natl. Acad. Sci. USA.* 83:9512–9516.

Dente, L., G. Cesarini, and R. Cortese. 1983. pEMBL: a new family of single stranded plasmids. *Nucleic Acids Res.* 11:1645–1655.

Edwards, K. A., R. A. Montague, S. Shepard, B. A. Edgar, R. L. Erikson,

and D. P. Kiehart. 1994. Identification of *Drosophila* cytoskeletal proteins by induction of abnormal cell shape in fission yeast. *Proc. Natl. Acad. Sci. USA.* 91:4589–4593.

Everett, A. W., and K. A. Nichol. 1990. Ezrin immunoreactivity in neuron subpopulation: cellular distribution in relation to cytoskeletal proteins in sensory neurons. *J. Histochem. Cytochem.* 38:1137–1144.

Fazioli, F., W. T. Wong, S. Ullrich, K. Sakaguchi, E. Appella, and P. Di Fiore. 1993. The ezrin-like family of tyrosine kinase substrates: receptor-specific pattern of tyrosine phosphorylation and relationship to malignant transformation. *Oncogene.* 8:1335–1345.

Funayama, N., A. Nagafuchi, N. Sato, Sa. Tsukita, and Sh. Tsukita. 1991. Radixin is a novel member of the band 4.1 family. *J. Cell Biol.* 115: 1039–1048.

Gary, R., and A. Bretscher. 1993. Heterotypic and homotypic associations between ezrin and moesin, two putative membrane-cytoskeletal linking proteins. *Proc. Natl. Acad. Sci. USA.* 90:10846–10850.

Gould, K. L., A. Bretscher, F. S. Esch, and T. Hunter. 1989. cDNA cloning and sequencing of the protein-tyrosine kinase substrate, ezrin, reveals homology to band 4.1. *EMBO (Eur. Mol. Biol. Organ.) J.* 8:4133–4142.

Gould, K. L., J. A. Cooper, A. Bretscher, and T. Hunter. 1986. The protein-tyrosine kinase substrate, p81, is homologous to a chicken microvillar core protein. *J. Cell Biol.* 102:660–669.

Goslin, K., E. Birgbauer, G. Banker, and F. Solomon. 1989. The role of cytoskeleton in organizing growth cones: a microfilament-associated growth cone component depends upon microtubules for its localization. *J. Cell Biol.* 109:1621–1631.

Gu, M., J. D. York, I. Warshawsky, and P. W. Majerus. 1991. Identification, cloning, and expression of a cytosolic megakaryocyte protein-tyrosine phosphatase with sequence homology to cytoskeletal protein 4.1. *Proc. Natl. Acad. Sci. USA.* 88:5867–5871.

Hanzel, D., H. Reggio, A. Bretscher, J. G. Forte, and P. Mangeat. 1991. The secretion-stimulated 80K phospho-protein of parietal cells is ezrin, and has properties of a membrane cytoskeletal linker in the induced apical microvilli. *EMBO (Eur. Mol. Biol. Organ.) J.* 10:2363–2373.

Hunter, T., and J. A. Cooper. 1981. Epidermal growth factor induces tyrosine phosphorylation of proteins in A431 human tumor cells. *Cell.* 24:741–752.

Kitts, P. A., and R. D. Possee. 1993. A method for producing recombinant baculovirus expression vectors at high frequency. *Biotechniques.* 14:810–817.

Krieg, J., and T. Hunter. 1992. Identification of the two major epidermal growth factor-induced tyrosine phosphorylation sites in the microvillar core protein ezrin. *J. Biol. Chem.* 267:19258–19265.

Knops, J., K. S. Kosik, G. Lee, J. L. Pardee, L. Cohen-Gould, and L. McConlogue. 1991. Overexpression of tau in a nonneuronal cell induces long cellular processes. *J. Cell Biol.* 114:725–733.

Lankes, W. T., and H. Furthmayr. 1991. Moesin: a member of the protein 4.1-talin-ezrin family of proteins. *Proc. Natl. Acad. Sci. USA.* 88:8297–8301.

Mangeat, P. H., T. Gusdinar, A. Sahuquet, D. K. Hanzel, J. G. Forte, and R. Magous. 1990. Acid secretion and membrane reorganization in single gastric parietal cell in primary culture. *Biol. Cell.* 69:223–232.

Martin, M., and P. Mangeat. 1994. Expression of rat H^+-K^+-ATPase in insect cells using a double recombinant baculovirus. *In* Molecular and Cellular Mechanisms of H^+ Transport. B. H. Hirst, editor. NATO ASI Series, subseries H "Cell Biology." Springer-Verlag, Berlin. 89:359–366.

Mercier, F., H. Reggio, G. Devilliers, D. Bataille, and P. Mangeat. 1989. A marker of acid-secreting membrane movement in rat gastric parietal cells. *Biol. Cell.* 65:7–20.

Norris, K., S. Rahbar, and R. B. Wallace. 1983. Efficient site-directed mutagenesis by simultaneous use of two primers. *Nucleic Acids Res.* 11: 5103–5112.

Parker, L. L., S. Atherton-Fessler, M. S. Lee, S. Ogg, J. L. Falk, K. I. Swenson, and H. Piwnica-Worms. 1991. Cyclin promotes the tyrosine phosphorylation of $p34^{cdc2}$ in a $wee1^+$ dependent manner. *EMBO (Eur. Mol. Biol. Organ.) J.* 10:1255–1263.

Rees, D. J. G., S. E. Ades, S. J. Singer, and R. O. Hynes. 1990. Sequence and domain structure of talin. *Nature (Lond.).* 347:685–689.

Rouleau, G. A., P. Merel, M. Lutchman, M. Sanson, J. Zucman, C. Marineau, K. Hoang-Xuan, S. Demczuk, C. Desmaze, B. Plougastel, et al. 1993. Alteration in a new gene encoding a putative membrane-organizing protein causes neuro-fibromatosis type 2. *Nature (Lond.).* 363:515–521.

Royer, M., S. S. Hong, B. Gay, M. Cerutti, and P. Boulanger. 1992. Expression and extracellular release of human immunodeficiency virus type 1 gag precursors by recombinant baculovirus-infected cells. *J. Virol.* 66:3230–3235.

Sato, N., N. Funayama, A. Nagafuchi, S. Yonemura, Sa. Tsukita, and Sh. Tsukita. 1992. A gene family consisting of ezrin, radixin and moesin. *J. Cell Sci.* 103:1–13.

Sato, N., S. Yonemura, T. Obinata, Sa. Tsukita, and Sh. Tsukita. 1991. Radixin, a barbed-end capping actin-modulating protein, is concentrated at the cleavage furrow during cytokinesis. *J. Cell Biol.* 113:321–330.

Takeuchi, K, A. Kawashima, A. Nagafuchi, and S. Tsukita. 1994*a*. Structural diversity of band 4.1 superfamily members. *J. Cell Sci.* 107:1921–1928.

Takeuchi, K., N. Sato, H. Kasahara, N. Funayama, A. Nagafuchi, S. Yonemura, Sa. Tsukita, and Sh. Tsukita. 1994*b*. Perturbation of cell adhesion and microvilli formation by antisense oligonucleotides to ERM family members. *J. Cell Biol.* 125:1371–1384.

Trofatter, J. A., M. M. MacCollin, J. L. Rutter, J. R. Murrell, M. P. Duryao, D. M. Parry, R. Eldridge, N. Kley, A. G. Menon, K. Pulaski, et al. 1993. A novel moesin-, ezrin-, radixin-like gene is a candidate for the neurofibromatosis tumor suppressor. *Cell.* 72:791–800.

Tsukita, Sa., Y. Hieda, and Sh. Tsukita. 1989. A new 82 kD barbed end-capping protein (radixin) localized in the cell-to-cell adherens junction: purification and characterization. *J. Cell Biol.* 108:2369–2382.

Tsukita., Sh., M. Itoh, A. Nagafuchi, Sh. Yonemura, and Sa. Tsukita. 1993. Submembranous junctional plaque proteins include potential tumor molecules. *J. Cell Biol.* 123:1049–1053.

Tsukita, Sa., K. Oishi, N. Sato, J. Sagar, A. Kawai, and Sh. Tsukita. 1994. ERM family members as molecular linkers between the cell surface glycoprotein CD44 and actin-based cytoskeletons. *J. Cell Biol.* 126:391–401.

Turunen, O., T. Wahlström, and A. Vaheri. 1994. Ezrin has a COOH-terminal actin-binding site that is conserved in the ezrin protein family. *J. Cell Biol.* 126:1445–1453.

Turunen, O., R. Winqvist, R. Pakkanen, K. H. Grzeschik, T. Wahlström, and A. Vaheri. 1989. Cytovillin, a microvillar Mr 75,000 protein. cDNA sequence, prokaryotic expression, and chromosomal localisation. *J. Biol. Chem.* 264:16727–16732.

Urushidani, T., D. K. Hanzel, and J. G. Forte. 1989. Characterization of an 80 kD phosphoprotein involved in parietal cell stimulation. *Am. J. Physiol.* 256:G1070–G1081.

Volkman, L. E., and K. J. M. Zaal. 1990. *Autographica californica* M nuclear polyhedrosis virus: microtubules and replication. *Virology.* 175:292–302.

Volkman, L. E., S. N. Talhouk, D. I. Oppenheimer, and C. A. Charlton. 1992. Nuclear F-actin: a functional component of baculovirus-infected lepidopteran cells? *J. Cell Sci.* 103:15–22.

Wollweber L., R. Stracke, and U. Gothe. 1980. The use of a simple method to avoid cell shrinkage during SEM preparation. *J. Microsc.* 121:185–189.

Yang, Q., and N. K. Tonks. 1991. Isolation of a cDNA clone encoding a human protein-tyrosine phosphatase with homology to the cytoskeletal-associated proteins band 4.1, ezrin, and talin. *Proc. Natl. Acad. Sci. USA.* 88:5949–5953.

Yao, X., A. Thibodeau, and J. G. Forte. 1993. Ezrin-calpain interactions in gastric parietal cells. *Am. J. Physiol.* 265 (*Cell Physiol.* 34):C36–C46.